Diffusive evolution of stable and metastable phases. II. Theory of nonequilibrium behavior in colloid-polymer mixtures

R. M. L. Evans* and W. C. K. Poon[†]

Department of Physics and Astronomy, The University of Edinburgh, JCMB King's Buildings, Mayfield Road, Edinburgh EH9 3JZ, United Kingdom

By analytically solving some simple models of phase-ordering kinetics, we suggest a mechanism for the onset of nonequilibrium behavior in colloid-polymer mixtures. These mixtures can function as models of atomic systems; their physics therefore impinges on many areas of thermodynamics and phase ordering. An exact solution is found for the motion of a single, planar interface separating a growing phase of uniform high density from a supersaturated low-density phase, whose diffusive depletion drives the interfacial motion. In addition, an approximate solution is found for the one-dimensional evolution of two interfaces, separated by a slab of a metastable phase at intermediate density. The theory predicts a critical supersaturation of the low-density phase, above which the two interfaces become unbound and the metastable phase grows *ad infinitum*. The growth of the stable phase is suppressed in this regime. [S1063-651X(97)03311-4]

PACS number(s): 82.70.Dd, 64.60.My, 05.70.Ln

I. INTRODUCTION

Metastability and phase transition kinetics in condensed matter are rapidly expanding fields of research [1,2]. Experimentally, it is increasingly realized that *colloidal systems* exhibit unique properties which make them attractive candidates for studying these topics. Advances in synthetic chemistry mean that suspensions of particles of well-characterized shapes and sizes, and with precisely tunable interparticle interactions, can be routinely produced. The *equilibrium* phase behavior of such model colloids can be studied experimentally and understood in some detail using the standard tools of statistical mechanics [3]. Moreover, colloids are much larger than atoms, the typical dimension of a colloid being $L \approx 0.5$ μm, and the solids they form (crystal, glass, and gel) are mechanically weak, a typical modulus being $G \sim k_B T/L^3 \approx 10^{-2}$ N m^{-2}. Thus a colloidal crystal can be ''shear melted'' to the metastable colloidal fluid state simply by shaking. Structural dynamics of colloidal systems are also slow, the scale being set by the time a free particle takes to diffuse its own dimension, $\tau_R \sim L^2/D$. Estimating the diffusion coefficient D by the Stokes-Einstein relation for a spherical particle of radius $L \sim 0.5$ μm suspended in a liquid of viscosity $\eta \sim 10^{-3}$ N m^{-2} s, we get $D = k_B T/6\pi\eta L \sim 4 \times 10^{-13}$ m^2 s^{-1}, so that the characteristic relaxation time in colloidal systems is $\tau_R \gtrsim 1$ s. Thus the crystallization of a metastable colloidal fluid can take minutes, hours, or even days. These two features, the ease with which metastable states can be prepared and the long relaxation times involved, mean that the study of phase transition kinetics and metastability in model colloids is gaining increasing attention. For example, there is a growing literature on crystallization kinetics in nearly-hard-sphere poly(methyl methacrylate) colloids [4]. The glass transition in the same system is now recognized as being one of the simplest examples of that phenomenon and has become a testing ground for sophisticated theories [5].

In recent work aimed at elucidating the equilibrium phase behavior of mixtures of nearly-hard-sphere colloids and nonadsorbing polymers, we have also observed a rich variety of nonequilibrium behavior [6,7]. The well-characterized nature of our experimental system, coupled with detailed data from small-angle light scattering [7], has allowed us to suggest a possible link between the onset of formation of nonequilibrium phases and the presence of a ''hidden,'' metastable minimum in the free-energy landscape. In this paper, we review the experimental evidence leading to this suggestion and model the kinetic consequences of such a three-minima free-energy landscape in one dimension using a continuum approach. We conclude by pointing to the possible applications of this model in other ''soft'' systems. Some of our work relies on results from the preceding paper [8]; the main ideas are summarized in [9].

II. NONEQUILIBRIUM BEHAVIOR IN COLLOID-POLYMER MIXTURES

Free polymer alters the phase behavior of colloids via the depletion mechanism [10]. Exclusion of polymer from the region between the surfaces of two nearby colloidal particles gives rise to an unbalanced osmotic pressure pushing the particles together, resulting in an attractive depletion potential U_{dep}. In the case of hard-sphere-like colloids, the total interparticle interaction [11] in the presence of polymers is given approximately by

$$U(r) = \begin{cases} +\infty & \text{for } r \leq \sigma \\ -\Pi_p(\mu_p)V_{\text{overlap}} = U_{\text{dep}} & \text{for } \sigma < r \leq \sigma + 2r_g \\ 0 & \text{for } r > \sigma + 2r_g, \end{cases} \tag{1}$$

where $\sigma = 2a$ is the particle diameter and $\Pi_p(\mu_p)$ is the osmotic pressure of the polymer as a function of the polymer

*Electronic address: r.m.l.evans@ed.ac.uk
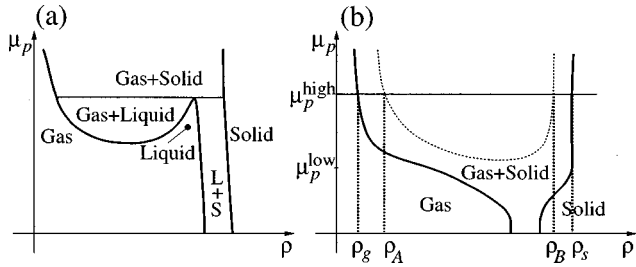
[†]Electronic address: w.poon@ed.ac.uk

FIG. 1. Phase diagrams of colloid-polymer mixtures in the colloid concentration (ρ) –polymer chemical potential (μ_p) plane, for size ratio ξ (a) above and (b) below ξ_{crit}. The dotted curve is a ''hidden'' gas-liquid binodal. For (b), the free-energy plots for two polymer chemical potentials, μ_p^{low} and μ_p^{high}, are shown in Figs. 2(a) and 2(b), respectively. The values of ρ for the various boundaries at $\mu = \mu_p^{\text{high}}$ are given by the common tangent construction in Fig. 2(b).

FIG. 2. Fluid and crystal branches of the free-energy density versus colloid volume fraction (a) at low polymer chemical potential [e.g., μ_p^{low} in Fig. 1(b)], when the fluid branch has a single minimum, and (b) at higher polymer chemical potential [e.g., μ_p^{high} in Fig. 1(b)], when two minima exist in the fluid branch, corresponding to gas and metastable liquid phases. The common tangent construction is used to find the densities of the coexisting equilibrium gas and solid phases (ρ_g, ρ_s), and the metastable gas-liquid and liquid-solid binodals (ρ_A, ρ_B) and (ρ_C, ρ_D); see Fig. 1(b).

chemical potential μ_p. V_{overlap} is the volume of the overlapping depletion zones between two particles at an intercenter separation of r. Explicitly

$$V_{\text{overlap}} = \left\{ 1 - \frac{3r}{2\sigma(1+\xi)} + \frac{1}{2}\left[\frac{r}{\sigma(1+\xi)}\right]^3 \right\} \frac{\pi}{6} \sigma^3 (1+\xi)^3, \tag{2}$$

where $\xi = r_g/a$ denotes the ratio of the radius of gyration of the polymer r_g to the radius of the colloidal particle a.

Theory [10] predicts and experiments [11] show that the phase diagram of a mixture of hard-sphere colloids and nonadsorbing polymer is a function of the size ratio ξ. The phase diagram at large enough ξ is reminiscent of that of a simple atomic substance [Fig. 1(a)], with the polymer chemical potential (μ_p) playing the role of an inverse temperature. (Temperature itself is not an axis of the phase diagram because, in systems with only excluded-volume interactions, no energy scale exists [12].) Colloidal gas, liquid, and crystal phases are possible, with regions of binary coexistence between pairs of these phases and triple coexistence at a particular value of μ_p. As the size ratio ξ is decreased, the region of colloidal gas-liquid coexistence shrinks until, below a critical value ξ_{crit}, the gas-liquid coexistence region disappears altogether from the equilibrium phase diagram [Fig. 1(b)]; now, only colloidal fluid or crystal phases exist in equilibrium. Experimentally, $\xi_{\text{crit}} \approx 0.25$.

Focus now on the phase diagram for the case of $\xi < \xi_{\text{crit}}$ [Fig. 1(b)]. Experiments confirm that moderate concentrations of a small nonadsorbing polymer cause a suspension of hard spheres to phase separate into coexisting colloidal fluid and crystal phases. At higher colloidal concentrations, or higher μ_p, across a *nonequilibrium boundary* (NEB), crystallization is suppressed [6], [7]. Instead, a variety of nonequilibrium aggregation behaviors is observed. Detailed small-angle light-scattering studies [7] have allowed the classification of the kinetic behavior above the NEB into three types. Just across the NEB, the behavior is ''nucleation-like.'' This is characterized by an initial latency period consistent with nucleation, after which dense, amorphous droplets separate out, forming an amorphous sediment that begins to crystallize only on a much longer time scale. The nucleationlike regime is of primary interest to us in this article. At
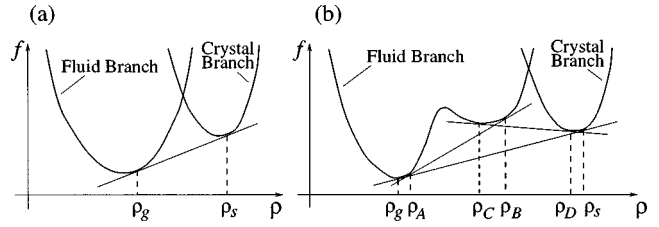
higher μ_p, or higher colloid concentration, the behavior becomes ''spinodal-like,'' switching finally to a ''transient gelation'' regime for the densest systems.

It should be stressed that the experimentally observed NEB is sharp and highly reproducible. In fact, it has been suggested by one of us [7] that this boundary is given by a hidden gas-liquid binodal. Following the theoretical approach in [10], we write the free energy $F(\rho, \mu_p)$ of a colloid-polymer mixture as a function of the colloid volume fraction (or ''density'') ρ and the polymer chemical potential μ_p. F can be calculated within a mean-field framework for a disordered arrangement of colloids and polymers, the ''fluid branch,'' and an ordered arrangement of colloids with polymers randomly dispersed, the ''crystal branch.'' At low polymer chemical potentials, the fluid and crystal branches both show a single minimum [Fig. 2(a)]. This gives rise to single-phase fluid ($\rho < \rho_g$), fluid-crystal coexistence ($\rho_g < \rho < \rho_s$), or single-phase crystal ($\rho > \rho_s$). The colloid concentrations in coexisting fluid and crystal phases are obtained by the common tangent construction (see, e.g., [13]).

At higher polymer chemical potentials, however, the fluid branch of the free energy shows a ''double minimum'' structure [Fig. 2(b)]. At larger polymer to colloid size ratios, this double minimum can give rise to a region of colloidal gas-liquid coexistence in the equilibrium phase diagram [Fig. 1(a)] [10,11]. For small polymers, however, the theory predicts only separation into fluid and crystal phases. Nevertheless, the ''metastable gas-liquid binodal,'' which is ''buried'' within the fluid-crystal coexistence region predicted by equilibrium thermodynamics, can still be traced out [Fig. 1(b)]. The equilibrium phase boundary and the metastable gas-liquid binodal, calculated using the theory in [10], compare well with the experimental equilibrium fluid-crystal coexistence boundary and the nonequilibrium boundary respectively [7], giving rise to the speculation that the suppression of crystallization, which is the predicted, equilibrium phase behavior, is linked to the presence of the hidden gas-liquid binodal.

In this and the preceding paper [8], we provide a theoretical basis for this speculation. We model the effects of a metastable third minimum in the free-companion energy curve on the kinetics of phase ordering, focusing on postnucleation kinetics. A system that has been homogenized (e.g., by shear melting) to some uniform density between ρ_g

and ρ_s (see Fig. 2) must evolve towards the equilibrium state, by separating into regions of density ρ_g and ρ_s. If $f(\rho)$ has positive curvature at the initial density, then the evolution begins by nucleation, whereby a thermal fluctuation causes part of the system to cross the barrier between the two stable wells in f. Once such a nucleus has formed (in the *early* stage of phase ordering), it grows by diffusively depleting the surrounding, supersaturated medium (the *growth* stage [14]).

In the preceding paper [8], we consider the implications for short-range (on the length scale of the transition zone between neighboring phases) density variations and stability, in the context of quasi-steady-state motion. There, and in Ref. [9], it is shown that an interface between regions of different densities may split, in the presence of a metastable minimum, into two parts. The purpose of the present article is to model the evolution of a split interface during the growth stage, considering large length scales (so interfaces appear as sharp steps, and relatively gentle concentration gradients control the diffusive dynamics) and time scales (so motion is time dependent, not steady state). We will find that growth dynamics involving split interfaces contrasts greatly with normal growth behavior.

The plan of this paper is as follows. The model introduced in Sec. III, involving a nucleus with an ordinary, unsplit interface, sets the scene for the methods employed. It is a completely soluble model for the motion of a single domain wall. The result agrees with that of Frank [15]. In Sec. IV, we analyze a more elaborate scenario, where two domain walls (the two parts of a ''split'' interface) enclose a region of metastable density and compete for the flux of condensing material. This model exhibits behavior consistent with the non-equilibrium boundary in the colloid-polymer phase diagram. The limitations of our work are discussed in Sec. V, while applications to related systems are given in Sec. VI.

In the models presented, growth is limited by diffusion of matter only. This simplification holds in many soft condensed systems, for which diffusion of latent heat is irrelevant since the entropy is dominated by the degrees of freedom of the solvent [12]. Moreover, we assume that the system may be described by a *single* conserved order parameter (such as the density of colloidal particles). Formally, this does not apply in colloid-polymer mixtures, where the polymer concentration is a second conserved quantity. However, it should be a reasonable model for small ξ, such that the polymers diffuse much more rapidly than the colloids. Non-conserved order parameters describing crystallinity are also omitted, under the assumption that such variables relax quickly compared with the diffusive order parameter and are therefore not rate limiting.

III. EXACT SOLUTION OF THE DIFFUSION EQUATION FOR TWO-PHASE SEPARATION

In this section, we find an exact solution of a problem pertinent to the intermediate- to late-stage evolution of a two-phase system. It is well known [14] that, when a dense droplet grows into a surrounding, supersaturated medium, the speed of motion of the interface is proportional to $t^{-1/2}$. We solve an idealized one-dimensional model for the motion of a single interface in such a situation and find the constant

of proportionality as a function of the supersaturation of the ambient medium. This problem was solved, using a different approach, by Frank [15]. Our solution by an alternative method is presented both for completeness and to introduce notation. The results obtained in this section will be used in Sec. IV to investigate the effect on interfacial motion of a ''metastable minimum'' in the free-energy landscape.

A. Idealized model

Consider an infinite, one-dimensional system whose equilibrium state is two-phase coexistence, which has been homogenized to a uniform density (e.g., by shear melting). In the system, a region of the high-density phase has nucleated at its equilibrium density and the interface between the high- and low-density phases has locally equilibrated. The domain wall proceeds to move by depleting the supersaturated low-density phase. Let the interface be located at $x = x_1(t)$ and let the density of the high-density phase be uniform at $\rho = \rho_s$. So the evolution of the system is solely due to the dynamics of the low-density region. In this phase, the density is ρ_g at the interface ($x = x_1$) and tends asymptotically to the supersaturated value $\rho_g + \sigma$ as $x \to \infty$. The assumption that the density (and hence chemical potential) is fixed at the equilibrium value [given by the double-tangent construction in Fig. 2(a)] at the interface is physically valid if the interface moves sufficiently slowly [8]. The problem of finding $x_1(t)$ is that of solving the diffusion equation

$$\frac{\partial \rho}{\partial t} = D \frac{\partial^2 \rho}{\partial x^2},$$

with boundary conditions $\rho(\infty, t) = \rho_g + \sigma$ and

$$\rho(x_1, t) = \rho_g, \tag{3}$$

with a moving boundary at $x_1(t)$, whose velocity depends on the flux at that point since, by conservation of matter at the interface,

$$(\rho_s - \rho_g)\, \dot{x}_1 = D \rho'(x_1). \tag{4}$$

The initial conditions are $x_1 = 0$ and $\rho(x > x_1) = \rho_g + \sigma$, with a singularity at $x = x_1$ (see the inset in Fig. 3) since $\rho(x_1) = \rho_g \forall t$. The system is depicted, at some later time t, in Fig. 3.

B. Solution

Solving the diffusion equation with a moving boundary (a Stefan problem) is difficult. The problem is overcome by replacing the semi-infinite region in which the diffusion equation is to be applied, by an infinite region, with a source or sink at x_1, whose strength $s(t)$ is such that the region $x > x_1$ cannot distinguish it from a moving interface. The behavior in $x < x_1$, which is just a construct of the method, should simply be ignored. The initial conditions in this region may be freely chosen to facilitate the solution. Let $\rho(x \neq x_1(0), t = 0) = \rho_g + \sigma$ and let y be defined as the deviation from this ambient density: $y = \rho - \rho_g - \sigma$. So the equation to be solved is the diffusion equation with a source at $x = x_1(t)$,
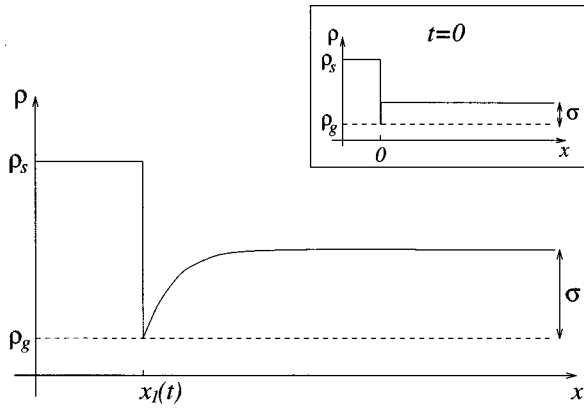
FIG. 3. Graph of density ρ against position x. On the left is the dense region that has been nucleated and is growing at the uniform density ρ_s, which is its equilibrium density. The interface is located at $x = x_1$, which is a function of time, since matter is flowing down the concentration gradient in the sparse phase and condensing onto the high-density region. At the base of the interface, the density is that of the coexisting gas ρ_g. The "ambient" density far from the interface is $\rho_g + \sigma$. Inset: the initial ($t=0$) configuration of the system, with a singularity at the base of the domain wall.

$$\frac{\partial y}{\partial t} = D\frac{\partial^2 y}{\partial x^2} - \delta(x - x_1(t))\, s(t), \tag{5}$$

with the wall position $x_1(t)$ and the construct $s(t)$ fixed by the boundary conditions. Equation (5) is solved by

$$y(x,t) = -\int_0^t dt' \int_{-\infty}^{\infty} dx'\; G(x-x',t-t')$$

$$\times\, \delta(x' - x_1(t'))s(t')$$

using the Green's function

$$G(x,t) = \frac{1}{\sqrt{4\pi D t}}\exp\left(\frac{-x^2}{4Dt}\right).$$

Hence the density field is given in terms of $s(t)$ and $x_1(t)$ by

$$\rho(x,t) = \rho_g + \sigma - \int_0^t dt'\, \frac{s(t')}{\sqrt{4\pi D(t-t')}}\exp-\frac{[x-x_1(t')]^2}{4D(t-t')}.$$

Applying Eqs. (3) and (4) gives us two integral equations in the two unknown functions $x_1(t)$ and $s(t)$, valid for all positive t:

$$\int_0^t dt'\, \frac{s(t')}{\sqrt{4D(t-t')}}\exp-\frac{[x_1(t)-x_1(t')]^2}{4D(t-t')} = \pi^{1/2}, \tag{6}$$

$$\int_0^t dt'\, \frac{[x_1(t)-x_1(t')]\, s(t')}{[4D(t-t')]^{3/2}}\exp-\frac{[x_1(t)-x_1(t')]^2}{4D(t-t')}$$

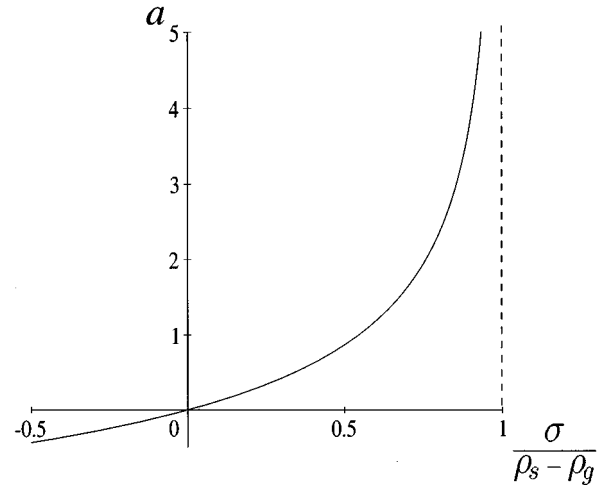$$= \frac{\pi^{1/2}(\rho_s-\rho_g)}{2D}\,\dot{x}_1(t). \tag{7}$$

FIG. 4. Velocity coefficient versus relative supersaturation.

The right-hand side of Eq. (6) is independent of t, and hence the t dependence must be removed from the exponential in the integrand. This requires

$$x_1(t) = a\sqrt{Dt} \tag{8}$$

and hence $s(t) = b\sqrt{(D/t)}$, where a and b are constants in time. Substituting into Eqs. (6) and (7) and evaluating the integrals (see the Appendix) results in a closed-form expression relating the coefficient a to the relative supersaturation,

$$\frac{\sigma}{\rho_s-\rho_g} = \frac{\sqrt{\pi}}{2}\,a e^{a^2/4}\mathrm{erfc}\,\frac{a}{2} \tag{9}$$

where erfc is the complementary error function, $\mathrm{erfc}\, x \equiv 1 - \mathrm{erf}\, x$. The coefficient b is not of particular interest, but we note that it is of the form $(\rho_s - \rho_g) \times$ [function of $\sigma/(\rho_s - \rho_g)$].

We have chosen to use the initial condition $x_1(0) = 0$ in deriving Eq. (8), but clearly the origin of x_1 is arbitrary since the physics is translation invariant and does not depend on the initial size of the dense region. The velocity of the interface, on the other hand, is well defined:

$$\dot{x}_1 = \frac{a}{2}\sqrt{\frac{D}{t}}. \tag{10}$$

Equation (10) lends a physical meaning to the coefficient a and so we will refer to it as the "velocity coefficient."

Equation (9) is plotted in Fig. 4 for a as a function of $\sigma/(\rho_s - \rho_g)$. The validity of the model extends to negative supersaturations, which result in evaporation of the dense phase and hence negative a. The curve plotted in Fig. 4 has no special features in the negative quadrant. As the relative supersaturation tends to negative infinity, the behavior of the velocity coefficient is given by

$$a \to -2\sqrt{\ln\left(\frac{-\sigma}{\rho_s-\rho_g}\right)}.$$

C. Linear and nonlinear regimes

For small relative supersaturation (close to the origin of Fig. 4), Eq. (9) tends to a linear relation

$$a \rightarrow \frac{2}{\sqrt{\pi}} \left(\frac{\sigma}{\rho_s - \rho_g} \right). \qquad (11)$$

From Eq. (4) we see that the flux *onto* the interface is $j_{\text{cond}} = (\rho_s - \rho_g) \dot{x}_1$. If we substitute Eqs. (10) and (11) into this expression, we see that the flux of material from the dilute phase condensing onto the interface is

$$j_{\text{cond}} \rightarrow \sigma \sqrt{D / \pi t} \qquad (12)$$

in the linear regime. This is independent of $\rho_s - \rho_g$ and depends only on properties of the dilute phase. So the condensation flux becomes independent of properties of the interface in this regime. The physics behind this statement is as follows. The density at the base of the interface is maintained at the constant value ρ_g and this gives rise to a gradient, and hence a flux, in the supersaturated dilute region. This gradient diminishes with time as material is depleted from the region, but is enhanced by the motion of the wall. It is clear from Fig. 3 that moving the wall to the right must accentuate the gradient. In the linear regime, the motion of the wall is slow enough for this enhancement of the gradient to be insignificant, and the flux onto the interface varies with time as if the boundary to the diffusive region were fixed. In Fig. 4 we see that the model gives rise to a divergence (albeit unphysical) of the velocity coefficient at a relative supersaturation of unity. The reason for this is now clear. At this supersaturation, the nonlinearity described above, whereby the interface motion enhances the gradient, becomes extreme. The interface can never deplete the ''low''-density region and hence the gradient (and therefore the flux) at its base remains infinite. Based on the exact solution of this simple model for interface motion [specifically Eq. (12)], we proceed to study a more elaborate situation.

IV. METASTABLE PHASE EVOLUTION BETWEEN TWO COMPETING INTERFACES

It was noted in Sec. II that the onset of nonequilibrium behavior in colloid-polymer mixtures seems to be connected with the appearance of a third minimum in the free-energy density, corresponding to a metastable liquid phase. Specifically, the formation of amorphous, nonequilibrium material from nucleationlike dynamics begins to occur at a supersaturation of the gas phase close to the hidden gas-liquid binodal. We now develop a model for the phase-ordering dynamics in systems with a third minimum of this kind.

In a system with such a three-well potential [such as that illustrated in Fig. 2(b)], three different species of interfaces may exist between regions of the various locally stable densities, during intermediate- to late-stage ordering. If the gas, metastable liquid, and solid phases are denoted g, l, and s, respectively, then g-l, l-s, and g-s interfaces may move through the system. If we use the ''equilibrium interface'' approximation, as applied in Sec. III, defining the densities above and below each interface to be the coexistence values for equilibrium between the two neighboring phases, then a
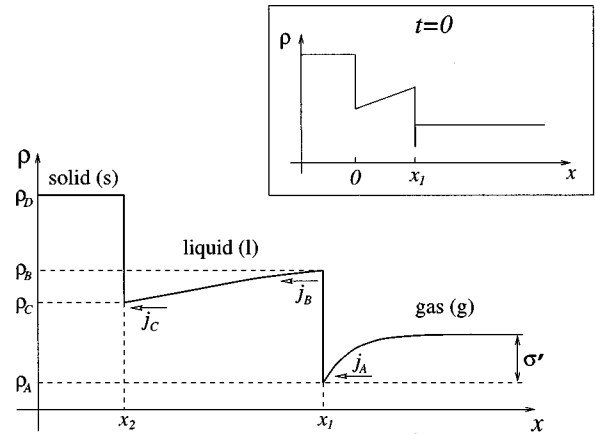

FIG. 5. Graph of density ρ against position x. The interface at x_1 separates the gas phase from the metastable liquid and is locally equilibrated so that the discontinuity in the density is between the metastable binodal values (ρ_A, ρ_B). The flux into (out of) the interface is j_A (j_B). The flux j_C of material of density ρ_C impinges on the interface at x_2, which separates the metastable liquid from the solid region of uniform density ρ_D. The ambient (i.e., asymptotic) density of the gaseous phase is the supersaturated value $\rho_A + \sigma'$. Inset: the initial configuration of the system, with a uniform gradient between the domain walls and a δ-function singularity in the gas phase at x_1.

g-s interface has the fixed densities (ρ_g, ρ_s), given by the double-tangent construction [13] in Fig. 2(b). Accordingly, at a g-l interface the densities are (ρ_A, ρ_B) and at an l-s interface, (ρ_C, ρ_D), which are the metastable coexisting values given in Fig. 2(b).

Consider the idealized system introduced in Sec. III, where a region of the dense solid has appeared in an otherwise homogeneous, supersaturated system. The ambient density is within the gas well of the bulk free-energy density. As before, the dense region will grow by depleting the supersaturated dilute region, but we can now imagine two alternative ways in which the growth can proceed. *Either* a g-s interface propagates into the dilute phase, and the system evolves as in Sec. III, *or* g-l and l-s interfaces form, and propagate separately, their motion being controlled by diffusion both in the ambient dilute region and in the intervening region of metastable liquid. Once formed, a g-s interface propagates stably with respect to small perturbations [8] and cannot easily be split into g-l and l-s parts. Hence, which of these two modes of growth the system exhibits depends on which was initiated at the nucleation stage. The criteria for which mode is initiated during nucleation in a given system are unknown at present, although there has been some conjecture [8,9]. Let us accept that the split-interface (g-l and l-s) mode of evolution has begun in our one-dimensional system and calculate the subsequent growth dynamics.

A. Model system

The density profile of the system in question, at some time t, is depicted in Fig. 5. The g-l interface is positioned at $x_1(t)$ and the constant densities ρ_A and ρ_B immediately adjacent to it are marked, as are the fluxes $j_A(t)$ and $j_B(t)$ in and out of the interface, which are defined in the direction of the arrows and are functions of time. The l-s interface is at

$x_2(t)$. The flux of material of density ρ_C into this interface is $j_C(t)$. There is no output flux, as the solid phase has a uniform density ρ_D. Let us make the model as general and physically realistic as possible by allowing different diffusion constants in the different phases: D_1 in the gaseous phase and D_2 in the metastable liquid. The supersaturated density at infinity is defined as $\rho_A + \sigma'$ in the figure. The ''adjusted supersaturation'' σ' is distinct from the supersaturation σ used in Sec. III. If the ambient (asymptotic) density is ρ_∞ then the supersaturation is the deviation of this density from the equilibrium value (the *stable* binodal), which is ρ_g in this system, i.e., $\sigma = \rho_\infty - \rho_g$. On the other hand, the *adjusted* supersaturation is the deviation from the metastable binodal, $\sigma' = \rho_\infty - \rho_A$.

Clearly, conservation of matter at the interfaces leads to the equations

$$(\rho_B - \rho_A)\dot{x}_1 = j_A - j_B, \tag{13}$$

$$(\rho_D - \rho_C)\dot{x}_2 = j_C. \tag{14}$$

Using these relations, we could proceed in the same manner as in Sec. III B, but this time solving two coupled diffusion equations. The diffusion equation for the gaseous region would have one source and that for the liquid region would have two. The strengths and positions of the sources would be fixed by Eqs. (13) and (14) and by fixing the constant densities ρ_A, ρ_B, and ρ_C. Equation (13) would couple the two equations. Proceeding in this manner to try to find an exact solution for the evolution of the system would lead to five coupled integro-differential equations in five unknown functions [$x_1(t)$, $x_2(t)$, and the strengths of three sources]. It is not easy to spot the solutions to this system of equations, as it was for Eqs. (6) and (7). Instead, we will make progress by introducing some physically reasonable approximations.

B. Approximations

The first approximation is to decouple the g-l interface from the gaseous driving region by using Eq. (12) for the input current:

$$j_A \approx \sigma' \sqrt{D_1 / \pi t}. \tag{15}$$

This becomes exact as $\sigma' \rightarrow 0$ and will presumably give *qualitatively* meaningful results at higher supersaturations, although with σ' becoming some *effective* supersaturation, deviating from the true value. We use σ' rather than σ in Eq. (15), as the boundary condition $\rho(x_1) - \rho_A = 0$ was used in its derivation.

As a second approximation let

$$j_B \approx j_C \approx D_2 \frac{\rho_B - \rho_C}{x_1 - x_2}, \tag{16}$$

which says that the gradient in the liquid region is approximately uniform. Intuitively, this seems to be a reasonable assumption. If we imagine that, at some time into the evolution, the positions of the interfaces could suddenly be frozen, then the liquid region would subsequently relax exponentially towards a uniform gradient. (Compare the related diffusion problem of the temperature profile in a conducting rod

with the ends held at different temperatures.) In this sense, the liquid region is constantly in a state of relaxation towards a uniform density gradient, for which Eq. (16) applies.

Let us define Δ to be the size of the metastable liquid region: $\Delta \equiv x_1 - x_2$. Then substituting Eqs. (15) and (16) in Eqs. (13) and (14) gives us the differential equation

$$\frac{d\Delta}{d(t/\tau)} = (t/\tau)^{-1/2} - \frac{\gamma}{2\Delta}, \tag{17}$$

with a constant

$$\tau \equiv \frac{\pi}{D_1} \left(\frac{\rho_B - \rho_A}{\sigma'} \right)^2 \tag{18}$$

which has units of (time)/(length)^2, and a dimensionless constant γ, which acts as an attractive coupling between the walls, given by

$$\gamma \equiv 2\pi \left(\frac{\rho_B - \rho_A}{\sigma'} \right)^2 \frac{D_2}{D_1} (\rho_B - \rho_C) \left(\frac{1}{\rho_B - \rho_A} + \frac{1}{\rho_D - \rho_C} \right). \tag{19}$$

The formula for γ is quite easy to understand. It is a ratio of quantities that drive the interfaces together (relating to diffusion in the metastable phase) to those that drive them apart (relating to the gaseous region). It is proportional to the ratio of the diffusion constants and to the difference in densities $(\rho_B - \rho_C)$ that drives flux through the liquid region. This difference is made dimensionless by the factor following it, which is dominated by the interface of smallest height. These quantities are divided by the square of the relative supersaturation, which is responsible for driving the g-l wall away from the l-s wall.

C. Solution

In Eq. (17), γ has a critical value of unity, above which the solution may be expressed parametrically as

$$\sqrt{t/\tau} = \frac{\Delta_0}{\sqrt{\gamma - 1}} \sin\theta \, \exp\frac{\theta}{\sqrt{\gamma - 1}},$$

$$\Delta = \frac{\Delta_0}{\sqrt{\gamma - 1}} (\sin\theta + \sqrt{\gamma - 1} \, \cos\theta) \, \exp\frac{\theta}{\sqrt{\gamma - 1}} \tag{20}$$

for values of the parameter θ in the range $0 \leqslant \theta \leqslant \pi - \arctan\sqrt{\gamma - 1}$. Here Δ_0 is the initial size of the metastable region. A critical value of γ implies [from Eq. (19)] a critical value σ_c of the adjusted supersaturation. The condition $\gamma > 1$ corresponds to $\sigma' < \sigma_c$. We see that a graph of Δ versus $\sqrt{t}$ is an affine deformation of a logarithmic spiral and the restricted domain of θ gives a branch thereof in the first quadrant. Hence the metastable region has a finite lifetime since Δ decays to zero at some positive value of t. We will refer to these solutions as ''diffusively bound,'' to distinguish from the tighter binding due to curvature energy in the Cahn-Hilliard model, which prevents a single g-s interface splitting into g-l and l-s parts [8]. Furthermore, there is no solution for $\Delta_0 = 0$. Hence, for $\sigma' < \sigma_c$, the flux of
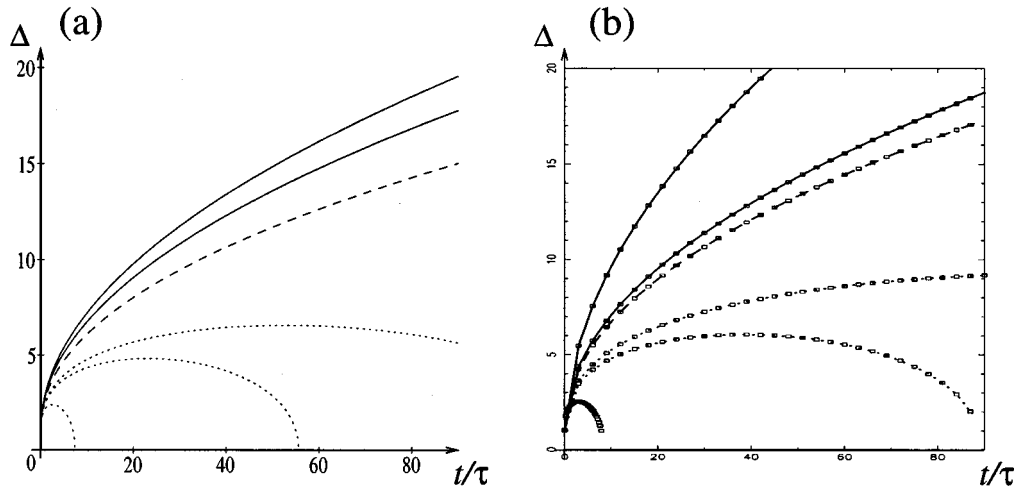
FIG. 6. (a) Size of the metastable region Δ [as given in Eqs. (20)–(22)] against time t in units of the constant τ, for various values of the coupling constant γ. Diffusively bound solutions are marked with a dotted line, for $\gamma=3$, $\gamma=2$, and $\gamma=1.8$. The marginal solution ($\gamma=1$) is dashed, and unbound solutions are plotted with solid lines, for $\gamma=0.8$ and 0.1. In each case, the initial size of the metastable region Δ_0 is unity. (b) Same plots, produced by numerical solution, without the approximations (15) and (16). The same values of γ are used as in (a).

condensation cannot, even momentarily, separate the g-l from the l-s wall if they are initially together. The diffusively bound solutions for Δ as a function of t/τ are plotted with dotted lines in Fig. 6(a) for various values of γ, with $\Delta_0=1$. Notice that the gradients of the curves are infinite where they meet each axis. The infinite gradient at $t=0$ arises from the infinite flux of condensing material due to the singularity in the density at the base of the g-l interface. At $\Delta=0$, the metastable region decays infinitely fast since the density gradient $(\rho_B-\rho_C)/\Delta$ diverges. Of course, in a physical situation, the gradient of $\Delta(t)$ would be flattened in both instances since the densities (ρ_A,ρ_B) do not truly remain constant for a fast-moving interface. Once the interfacial separation collapses to zero, the model breaks down. In a real system, the interfaces would combine into a single, stable g-s interface, which would continue to advance.

At the critical value $\gamma=1$, Eq. (17) has the parametric solution

$$\sqrt{t/\tau}=\Delta_0(\phi+1)\,\exp\phi,$$

$$\Delta=\Delta_0\phi\,\exp\phi, \qquad (21)$$

and for $\gamma<1$ (i.e., above the critical supersaturation), the solution is

$$\sqrt{t/\tau}=\frac{\Delta_0}{\sqrt{1-\gamma}}\sinh\phi\,\exp\frac{\phi}{\sqrt{1-\gamma}},$$

$$\Delta=\frac{\Delta_0}{\sqrt{1-\gamma}}(\sinh\phi+\sqrt{1-\gamma}\cosh\phi)\,\exp\frac{\phi}{\sqrt{1-\gamma}}, \qquad (22)$$

with $0\leq\phi<\infty$ in each case. Graphs of Δ versus t/τ, with $\Delta_0=1$, are plotted in Fig. 6(a), with solid lines for $\gamma<1$ and a dashed line for $\gamma=1$. These solutions are not bound, i.e., $\Delta>0$ for all positive t and $\Delta\to\infty$ as $t\to\infty$. So, above the critical supersaturation, the flux of condensing material, al-

though always dwindling, is sufficient to separate the g-l from the l-s interface, causing the metastable liquid phase to grow *ad infinitum*. This is even true in the extreme case where $\Delta_0=0$, when the solution becomes

$$\Delta=(1+\sqrt{1-\gamma}\,)\sqrt{t/\tau}\quad\text{for }\gamma\geq1. \qquad (23)$$

Equation (23) is also the limit of Eq. (22) as $t\to\infty$, so the size of the metastable region at late times is independent of its initial value.

To check the validity of Eqs. (15) and (16), we have numerically solved the system described in Sec. IV A (*without* the approximations made in Sec. IV B). The results plotted in Fig. 6(b) are for $D_2/D_1=0.1$. The variation of γ was controlled by varying σ' only. These results compare well with the approximate, closed-form solutions in Fig. 6(a). The same qualitative features (open or closed trajectories) appear and the critical value of γ is close to unity. The lifetimes of the bound solutions (which are very sensitive to the system parameters) agree to within a few percent for systems not too close to criticality. For the topmost trajectory in Fig. 6(b), $\sigma'/(\rho_B-\rho_A)\approx50\%$ so some deviation from linearity [Eq. (15)] is to be expected (see Sec. III C). We conclude that Eqs. (15) and (16) are quantitatively reasonable, and qualitatively very good, approximations.

In summary, the asymptotic (late-time or long-distance) behavior of a metastable region, for a system in which a double interface has formed early in the phase ordering, is as follows. For an ambient supersaturation σ' below the critical value

$$\sigma_c=(\rho_B-\rho_A)\sqrt{2\pi(\rho_B-\rho_C)\left(\frac{1}{\rho_B-\rho_A}+\frac{1}{\rho_D-\rho_C}\right)\frac{D_2}{D_1}}, \qquad (24)$$

there is no asymptotic behavior since the metastable region collapses in a finite time and subsequent evolution is via the ordinary g-s mode of interface propagation. Above the criti-

cal supersaturation, the metastable phase grows with time, according to Eq. (23). Notice, with reference to Fig. 2(b), that $\rho_B-\rho_C$ is a measure of the metastability of the liquid phase. Hence, at the triple point, when the three wells have a single common tangent, the critical supersaturation given by Eq. (24) goes to zero. In other words, at the triple point, no supersaturation is required to stabilize the liquid phase, so the physics is modeled successfully in this respect.

So far, we have concentrated on the size Δ of the metastable region, but the growth of the solid region is also of interest. For the double-interface mode of evolution, the size of the solid region is given, from Eqs. (14) and (16), by

$$x_2(t)=\left(\frac{\rho_B-\rho_C}{\rho_D-\rho_C}\right)D_2\int_0^t\frac{dt'}{\Delta(t')}.$$

Substituting the asymptotic expression for Δ [Eq. (23)] into this formula and using Eq. (18) for τ gives the result

$$x_2=\frac{2\sqrt{\pi}}{(1+\sqrt{1-\gamma})}\frac{D_2}{\sqrt{D_1}}\left(\frac{\rho_B-\rho_C}{\rho_D-\rho_C}\right)\left(\frac{\rho_B-\rho_A}{\sigma'}\right)\sqrt{t}.$$

Notice that this is *inversely* proportional to the (adjusted) supersaturation. It is interesting to compare this with the size of a solid region produced by normal interface motion (i.e., by a single g-s interface). To compare like with like, we should use the linearized velocity coefficient [Eq. (11), with $\rho_B-\rho_A$ replaced by $\rho_s-\rho_g$ for the interface height] together with Eq. (8). Denoting the size of the solid region produced by *single* interface motion by x_{sing}, we find

$$x_{\text{sing}}=\frac{2}{\sqrt{\pi}}\left(\frac{\sigma}{\rho_s-\rho_g}\right)\sqrt{D_1 t}.$$

Let ζ be the ratio of the size of the solid region produced by the double-interface mode of growth x_2 to that produced by normal growth x_{sing}. Then

$$\zeta=\frac{\pi}{1+\sqrt{1-\gamma}}\left(\frac{\rho_B-\rho_A}{\sigma'}\right)\left(\frac{\rho_s-\rho_g}{\sigma}\right)\frac{D_2}{D_1}\frac{\rho_B-\rho_C}{\rho_D-\rho_C}.$$

There is a distinct similarity between this formula and the expression for γ [Eq. (19)]. If we approximate $(\rho_D-\rho_A)+(\rho_B-\rho_C)$ by $\rho_s-\rho_g$, which we see, from Fig. 2(b), is usually a good approximation, then we find

$$\zeta\approx\frac{\gamma}{2(1+\sqrt{1-\gamma})}\frac{\sigma'}{\sigma}.$$

Since $0<\gamma<1$ for the split-interface mode of growth and also $\sigma'<\sigma$, it follows that

$$\zeta<\frac{\gamma}{2} \tag{25}$$

and that, well above the critical supersaturation, $\zeta\approx\gamma/4$.

Let us recapitulate the properties of the parameter γ. It appeared in Eq. (17) as an attractive coupling between the g-l and l-s interfaces. It is the ratio of properties of the liquid phase, tending to attract the interfaces, to properties of the
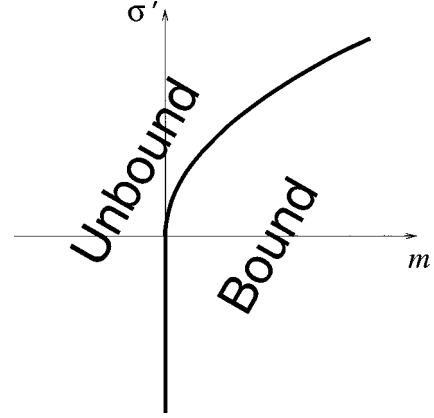

FIG. 7. Regions of metastability $m\equiv\rho_B-\rho_C$ and adjusted supersaturation σ' for which interfaces are diffusively bound or unbound.

gaseous phase, tending to separate them. It characterizes the classes of solutions of Eq. (17), being greater than unity for diffusively bound solutions and less than unity for unbound solutions. Finally, we see in Eq. (25) that it gives an upper bound (and an order of magnitude) for the ratio of growth rates of the solid phase in the split and normal modes of growth. Since $\gamma<1$ when the split mode occurs, Eq. (25) shows that this mode of evolution *suppresses* the growth of the solid.

Note that, in Fig. 2(b), the metastability of the middle well leads to the inequality $\rho_B>\rho_C$. If this liquid well were stable (i.e., below the double tangent to the outer two wells), the inequality would be violated. Hence it is reasonable to define the *metatability m* of the middle well to be $m\equiv\rho_B-\rho_C$. With reference to Eq. (24), we see that the boundary between regions of the (m,σ') plane, for which the g-l and l-s interfaces are diffusively bound or unbound, is of the form shown in Fig. 7. A naive expectation would be for a boundary coincident with the vertical axis, but we see that this is not the case. [For negative σ', for which the liquid phase *must* dissolve into the gas, we find solutions of Eq. (17) are again given by Eqs. (20)–(22), but with different ranges of the parameters θ and ϕ leading to closed trajectories whenever $\gamma>0$.]

V. DISCUSSION

Some nonequilibrium effects in colloid-polymer mixtures have been reviewed in Sec. II. We have remarked on the presence of a well-defined nonequilibrium boundary in the phase diagram, close to the theoretically calculated position of the hidden gas-liquid metastable binodal. This metastable binodal is central to the theoretical model developed in Sec. IV, where the position of its low-density branch was denoted by ρ_A. A system homogenized by shear melting to an ambient density of exactly ρ_A would, in the notation of Sec. IV, have a vanishing adjusted supersaturation $\sigma'=0$. In the model, this value has the special significance that, for $\sigma'>0$, a region of metastable liquid has an initial period of growth, before it collapses. At lower densities, any liquid region that is nucleated will immediately shrink. In experimental samples with a colloidal density above the nonequilibrium line in the phase diagram, the growth of crystals is

observed to be suppressed. This happens in the model for $\sigma' > \sigma_c$.

In practice, the lines $\sigma' = 0$ (the metastable binodal) and $\sigma' = \sigma_c$ may be experimentally indistinguishable, for two reasons. First, no very accurate theoretical prediction exists for the position of the metastable binodal in the phase diagram. Attempting to make quantitative comparisons of time scales with experiment, using the best available theories for the values of ρ_A, ρ_B, ρ_C, and ρ_D, results in uncertainties of several hundred percent in the value of γ. Second, the line $\sigma' = \sigma_c$ may be very close to the metastable binodal if σ_c is small. [From Eq. (24), this would occur if, e.g., the middle well in the potential were only slightly metastable or if the diffusion constant were much lower in the liquid than in the gas.] If σ_c is small then, writing $\gamma = (\sigma_c/\sigma')^2$ for $\rho_B > \rho_C$, we see that γ will decrease rapidly with increasing colloidal density and so, from Eq. (25), suppression of crystal growth will be pronounced at densities not far from the metastable binodal.

It seems, then, that the model presented here provides a plausible theoretical basis for the previous conjecture that the onset of nonequilibrium behavior in certain colloid-polymer mixtures is associated with the presence of a hidden gas-liquid binodal. It is, however, a greatly simplified and idealized picture and we should consider the ways in which it deviates from reality, and the implications for the resultant interfacial dynamics.

The model is one dimensional and therefore ignores surface tension. This is justifiable since, once a region has grown considerably larger than the critical nucleus size, surface tension has a negligible effect on interfacial motion during the growth stage [14]. It is at these intermediate to late times that our model describes the system. Dimensionality is also relevant to the time dependence of the long-range diffusion. This will have a quantitative effect on the predicted values of the critical supersaturation and the degree of suppression of crystal growth, etc. but we may conjecture that the qualitative features of the model's behavior will extend to three dimensions. The fact that our one-dimensional model does not explicitly address intrinsically higher-dimensional geometric effects, such as the Mullins-Sekerka instability [16], may not be important. The model gives us the general rule of thumb that, above a certain critical supersaturation, the crystalline regions (whatever shapes they may be), which would normally grow in a two-well system, are replaced, in the presence of a third well, by a metastable liquid. Subsequent to this growth stage, the metastable liquid is slowly transmuted into the "correct" equilibrium phase, i.e., crystal.

Probably a more drastic simplification is the semi-infinite extent of the ambient gaseous region in the model. In reality, there is more than one nucleus of the solid phase. There will be some typical internucleus spacing L_{nuc} in the system. The concentration profile in the gaseous region has a characteristic length scale $\sqrt{D_1 t}$, so when this is of order L_{nuc}, the nuclei begin to influence each other. After this time, the effective asymptotic supersaturation begins to fall, as the regions of depletion of the gas phase around the nuclei begin to overlap. This characteristic time to deplete the supersaturation of the gaseous phase may be denoted t_{dep} ($\sim L_{nuc}^2/D_1$). At this point, the metastable region around each nucleus is of

size $\Delta(t_{dep})$, which is given in Eq. (23). The remaining lifetime of the metastable regions may be calculated from Eqs. (20), as the time for a region initially of this size to collapse, in a system with adjusted supersaturation of zero. The total lifetime of the metastable phase is thus of order t_{dep}/γ. (Compare this with the naive calculation for a semi-infinite gaseous region, which gives a suppression of size of the solid region by a factor of order γ, and hence a time scale factored by $1/\gamma^2$, rather than $1/\gamma$.) We note that if σ_c is small, then the lifetime of the metastable phase $(\sigma'/\sigma_c)^2 t_{dep}$ grows rapidly with the ambient density. Once the metastable regions have collapsed and g-s interfaces form, the densities will diffusively readjust from ρ_A and ρ_D to ρ_g and ρ_s, in a relatively short time.

This whole discussion assumes that all interfaces in the system are undergoing the split mode of propagation (i.e., with g-l and l-s parts not bound together by curvature, as discussed in Sec. IV and Ref. [8]). Any "normal" (g-s) interfaces initiated in the system during nucleation will lead to the formation of large crystals on normal diffusive time scales. Such crystals are not observed experimentally above the nonequilibrium boundary. Therefore, our model is a good candidate for the physics of the nonequilibrium boundary *if*, for some reason, only split interfaces are generated during nucleation above this boundary. Such a scenario is not unreasonable. We have seen that diffusively bound interfaces are unbound by a sufficiently large supersaturation. It seems likely [8] (and has in fact been observed in a preliminary numerical study [9]) that a g-s interface (which is stabilized, or "bound" by a contribution to the chemical potential of the form $-\nabla^2\rho$) may be split or "unbound" in a manner analogous to diffusive unbinding and, furthermore, that the critical supersaturation to cause this is close in magnitude to that calculated here. This conjecture is based on the fact that, in a model that includes an extra $\nabla^2\rho$ term in the chemical potential to describe curvature effects (such as the Cahn-Hilliard model), the curvature term exactly balances the diffusive term in an equilibrium interface and hence quantities calculated from it will, in the main, be of the same order of magnitude as those calculated from the diffusive term only.

VI. RELATED SYSTEMS

The model we have investigated in this paper was originally suggested by experimental observations in mixtures of *spherical* colloids and nonadsorbing polymers of a substantially smaller size. The same model may, however, be applicable to other experimental systems.

First of all, it has been pointed out recently by one of us that the hidden binodal is probably significant for understanding the crystallization of globular proteins [17]. The kinetic predictions of this paper may therefore also be relevant in that context.

Furthermore, our model is probably directly relevant to mixtures of *rodlike* colloids and nonadsorbing polymers [18]. The two possible phase diagram topologies for this system are again those given in Figs. 2(a) and 2(b), but with the labels gas, liquid, and solid replaced by I_1, I_2, and N (standing for isotropic phases 1 and 2 and the nematic phase). Once more, three-phase coexistence disappears when the size of the polymer (relative now to the rod length) decreases
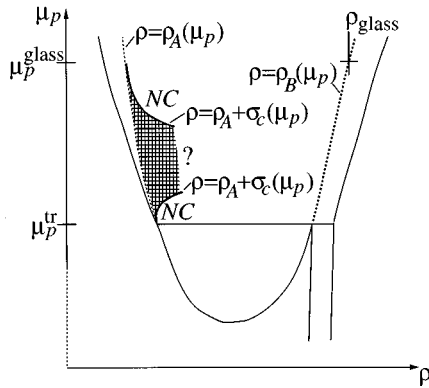
FIG. 8. Phase diagram in Fig. 1(a) redrawn schematically to emphasize the portion above the triple coexistence line at μ_p^{tr}. Here, within the equilibrium gas plus solid coexistence region, the metastable gas-liquid binodal is the dotted lines $\rho = \rho_A(\mu_p)$ and $\rho = \rho_B(\mu_p)$. The bold curves indicate the likely positions of parts of the diffusive unbinding boundary $\rho = \rho_A + \sigma_c(\mu_p)$. Near the triple coexistence line, the boundary meets the gas branch of the metastable binodal because the liquid well in the free-energy density is only marginally metastable. At μ_p^{glass}, the liquid branch of the metastable binodal reaches the vitrification density ρ_{glass}. In this vicinity, the critical supersaturation curve is again close to the gas branch of the metastable binodal, now because of the vanishing diffusion constant in the liquid phase. *NC* indicates regions where we expect disruption of crystallization, while normal gas-crystal coexistence is expected in the hatched area.

below a critical value. In this case [compare Fig. 2(b)], the addition of sufficient polymer to a suspension of rods leads to slow phase separation into an isotropic and a denser, coexisting nematic phase, the latter being distinguished by strong birefringence. Further addition of polymers, however, brings about a different kind of behavior: A weakly birefringent, "expanded" phase, which contains most of the rodlike particles, separates out quickly [19]. It has been suggested [19] that the suppression of isotropic-nematic phase separation is due to the presence of a hidden isotropic-isotropic binodal.

Let us return to spherical colloid and polymer mixtures. In the previous sections, we have concentrated on polymer-colloid size ratios ξ sufficiently small for no liquid phase to appear in the equilibrium phase diagram [Fig. 1(b)]. Now consider the case where the polymer is large enough to give rise to a thermodynamically stable gas-liquid binodal, as appears in Fig. 1(a). Note that, in the "gas + solid" region of Fig. 1(a), the form of $f(\rho)$ is as sketched in Fig. 2(b) and hence the model set up in this paper is again relevant. An expanded version of the phase diagram near the triple line, now showing the metastable portions of the gas-liquid binodal, is sketched in Fig. 8. As the triple line is approached from above ($\mu \to \mu_p^{tr}$), where the liquid well is only just metastable, the critical supersaturation vanishes ($\sigma_c \to 0$) because $\rho_B - \rho_C \to 0$; see Fig. 2(b) and Eq. (24). At higher values of μ_p, we expect another regime where $\sigma_c \to 0$, this time due to the vanishing of the diffusion coefficient in the liquid phase D_2 [see Eq. (24)]. As μ_p increases, the density of the metastable liquid phase ρ_B also increases; eventually $\rho_B \to \rho_{glass}$, the density at which the system vitrifies, with $D_2 \to 0$.

We can thus speculate on the form of the boundary for diffusive unbinding, $\rho = \rho_A(\mu_p) + \sigma_c(\mu_p)$, in the vicinity of the gas branch of the metastable binodal (Fig. 8). The prediction is that, for moderate colloid densities, there should be a region of suppressed crystallization immediately above the triple coexistence line (due to the very marginal metastability of the liquid minimum in the free-energy density) followed, for higher μ_p, by normal crystallization behavior and ending up with crystallization suppression again at the highest values of μ_p (due to the vitrification of the metastable liquid phase). Experimentally, the former nonequilibrium region has not been observed [11]. A search for this phenomenon is under way in our laboratory. However, the region of normal crystallization has been reported, as has a nonequilibrium boundary at higher μ_p [11], where it has been suggested [20] that vitrification of a dense phase does play a crucial role.

We speculate that the theoretical results contained in this paper should have some relevance to a number of other complex fluid systems in which metastability is known to play a key role in phase transformations, including the crystallization of the "monotropic liquid crystal," poly-*n*-nonyl-4-4'-biphenyl-2-chloroethane, via an intermediate, metastable nematic phase [21] and the crystallization of poly(phenylene ether) in cyclohexanol, where deep quenches produces first a fluid-fluid phase separation [22]. We acknowledge, however, that the limitations of our model discussed in Sec. V, together with the likelihood that latent heat may not be negligible in at least some instances, necessitates further research before reaching firm conclusions on its applicability.

VII. CONCLUSION

We have studied a simple model for diffusion-limited kinetics of phase ordering in a system whose free-energy density has a metastable third well, at a density intermediate to the two equilibrium phases. In such systems, we have found a mechanism whereby a region of the metastable phase may grow *ad infinitum* at the expense of the equilibrium dense phase if the mean density of the system is above a critical threshold. This behavior appears to be consistent with the nonequilibrium ordering dynamics and suppression of crystal growth observed experimentally in colloid-polymer mixtures. In the experimental system, as in the theoretical model, the onset of anomalous behavior occurs at a well-defined density.

The important lesson of this study (and the preceding paper [8]) is that any pair of concentrations, which can be linked by a double tangent on the graph of free-energy density versus concentration, may give rise to an interface in the evolving system. Although only the globally stable binodal densities will coexist in the equilibrated system, local and transient coexistence can occur between *any* binodal pairs of densities in a system that has not yet discovered its global equilibrium state. Hence metastable phases cannot be overlooked when modeling phase ordering. Indeed, their importance has long been accepted on an empirical level, particularly in a metallurgical context [23,13]. Ostwald's "rule of stages," for example [24], asserts that the transformation from one stable phase to another proceeds via all metastable

intermediates in turn. We have, in the present paper, a rationale for the consideration of such phases in a soft condensed matter setting.

APPENDIX A: EVALUATION OF INTEGRALS

Dividing Eq. (6) by Eq. (7) and using the appropriate functional forms for $x_1(t)$ and $s(t)$, and the substitution $t' = u^2 t$ to eliminate dimensionality from the integrands, we find the relation between the velocity coefficient and the relative supersaturation $\sigma/(\rho_B - \rho_A) = I_1/I_2$ where

$$I_1 \equiv \int_0^1 \frac{du}{\sqrt{1-u^2}} \exp{-\frac{a^2(1+u)}{4(1-u)}},$$

$$I_2 \equiv \int_0^1 \frac{du}{(1-u)\sqrt{1-u^2}} \exp{-\frac{a^2(1+u)}{4(1-u)}}.$$

Making a further change of variables $v^2 = (1+u)/(1-u)$ yields

$$I_2 = \int_1^\infty e^{-a^2 v^2/4} dv = \frac{\sqrt{\pi}}{a} \operatorname{erfc} \frac{a}{2},$$

$$I_1 = 2 \int_1^\infty \frac{e^{-a^2 v^2/4}}{1+v^2} dv = 2 e^{a^2/4} \int_1^\infty \frac{e^{-(a^2/4)(1+v^2)}}{1+v^2} dv.$$

We see that I_1 and I_2 are related by a derivative

$$\frac{d}{da}(I_1 e^{-a^2/4}) = -a I_2 e^{-a^2/4}.$$

Hence I_1 is given by the indefinite integral

$$I_1 = -\sqrt{\pi} e^{a^2/4} \int e^{-a^2/4} \operatorname{erfc} \frac{a}{2} \, da,$$

whose constant of integration is set by noting that I_1 vanishes as $a \to \infty$. This integral is soluble by parts, using

$$\int \operatorname{erfc} x \, dx = x \operatorname{erfc} x - \frac{e^{-x^2}}{\sqrt{\pi}} + \text{const.}$$

The solution is

$$I_1 = \frac{\pi}{2} e^{a^2/4} \left(\operatorname{erfc} \frac{a}{2} \right)^2,$$

from which Eq. (9) follows.

[1] J. M. Gunton, M. San Miguel and P. S. Sahni, in *Phase Transitions and Critical Phenomena*, edited by C. Domb and J. L. Lebowitz (Academic, London, 1983), Vol. 8, Chap. 3.
[2] A. J. Bray, Adv. Phys. **43**, 357 (1994).
[3] W. C. K. Poon and P. N. Pusey, in *Observation, Prediction and Simulation of Phase Transitions in Complex Fluids*, edited by M. Baus, L. F. Rull, and J.-P. Ryckaert (Kluwer, Dordrecht, 1995), p. 3.
[4] Y. M. He, B. J. Ackerson, W. van Megen, S. M. Underwood, and K. Schatzel, Phys. Rev. E **54**, 5286 (1996).
[5] W. van Megen and S. M. Underwood, J. Phys.: Condens. Matter **6**, A181 (1994).
[6] P. N. Pusey, A. D. Pirie, and W. C. K. Poon, Physica A **201**, 322 (1993).
[7] W. C. K. Poon, A. D. Pirie, and P. N. Pusey, Faraday Discuss. **101**, 65 (1995).
[8] R. M. L. Evans and M. E. Cates, preceding paper, Phys Rev. E **56**, 5738 (1997).
[9] R. M. L. Evans, W. C. K. Poon, and M. E. Cates, Europhys. Lett. **38**, 595 (1997).
[10] H. N. W. Lekkerkerker, W. C. K. Poon, P. N. Pusey, A. Stroobants, and P. B. Warren, Europhys. Lett. **20**, 559 (1992).
[11] S. M. Ilett, A. Orrock, W. C. K. Poon, and P. N. Pusey, Phys. Rev. E **51**, 1344 (1995).
[12] H. Löwen, Phys. Rep. **237**, 249 (1994).
[13] R. T. DeHoff, *Thermodynamics in Material Science* (McGraw-Hill, New York, 1993).
[14] M. Tokuyama and Y. Enomoto, Phys. Rev. E **47**, 1156 (1993).
[15] F. C. Frank, Proc. R. Soc. London, Ser. A **201**, 586 (1950).
[16] W. Mullins and R. F. Sekerka, J. Appl. Phys. **44**, 323 (1963).
[17] W. C. K. Poon, Phys. Rev. E **55**, 3762 (1997).
[18] H. N. W. Lekkerkerker, P. Buining, J. Buitenhuis, G. J. Vroege, and A. Stroobants, in *Observation, Prediction and Simulation of Phase Transitions in Complex Fluids*, edited by M. Baus, L. F. Rull, and J.-P. Ryckaert (Kluwer, Dordrecht, 1995), p. 53.
[19] M. P. B. van Bruggen, F. M. van der Kooij, and H. N. W. Lekkerkerker, J. Phys.: Condens. Matter **8**, 9451 (1996).
[20] N. A. M. Verhaegh, H. N. W. Lekkerkerker, D. Asnaghi, M. Giglio and L. Cipelletti, Physica A (to be published).
[21] D. Heberer, A. Keller, and V. Percec, J. Poly. Sci. Part B **33**, 1877 (1995).
[22] S. Berghmans, J. Mewis, H. Berghmans, and H. Meiger, Polymer **36**, 3085 (1995).
[23] J. W. Cahn, Trans. Metall. Soc. AIME **242**, 166 (1968).
[24] W. Ostwald, Z. Phys. Chem. (Munich) **22**, 286 (1897).